

Effect of substrate temperature on the growth and properties of boron-doped microcrystalline silicon films^{*}

Lei Qing-Song(雷青松)^{a)†}, Wu Zhi-Meng(吴志猛)^{a)}, Geng Xin-Hua(耿新华)^{b)},
Zhao Ying(赵颖)^{b)}, Sun Jian(孙健)^{b)}, and Xi Jian-Ping(奚建平)^{a)}

^{a)}*Institute of Micro and Nano Science and Technology, Shanghai Jiaotong University, Shanghai 200030, China*

^{b)}*Institute of Photo-Electronics, Nankai University, Tianjin 300071, China*

(Received 16 May 2005; revised manuscript received 22 September 2005)

Highly conductive boron-doped hydrogenated microcrystalline silicon ($\mu\text{c-Si:H}$) films are prepared by very high frequency plasma enhanced chemical vapour deposition (VHF PECVD) at the substrate temperatures (T_S) ranging from 90°C to 270°C. The effects of T_S on the growth and properties of the films are investigated. Results indicate that the growth rate, the electrical (dark conductivity, carrier concentration and Hall mobility) and structural (crystallinity and grain size) properties are all strongly dependent on T_S . As T_S increases, it is observed that 1) the growth rate initially increases and then arrives at a maximum value of 13.3 nm/min at $T_S=210^\circ\text{C}$, 2) the crystalline volume fraction (X_c) and the grain size increase initially, then reach their maximum values at $T_S=140^\circ\text{C}$, and finally decrease, 3) the dark conductivity (σ_d), carrier concentration and Hall mobility have a similar dependence on T_S and arrive at their maximum values at $T_S=190^\circ\text{C}$. In addition, it is also observed that at a lower substrate temperature T_S , a higher dopant concentration is required in order to obtain a maximum σ_d .

Keywords: boron-doped $\mu\text{c-Si:H}$ films, VHF PECVD, crystallinity, carrier concentration, Hall mobility

PACC: 8115G, 8155H, 6855

1. Introduction

P-layers are of great importance to the performance of silicon thin film solar cells.^[1,2] In order to achieve a perfect solar cell performance, high optical transmittance and high conductivity for p-layers are required. Studies have indicated that boron-doped $\mu\text{c-Si:H}$ films are an attractive alternative in the sense of their high doping efficiency, high electrical conductivity, and low optical absorption.^[3-5] This type of material has now been used in solar cells to improve the photovoltaic performance.^[1,6] The films are usually prepared by conventional radio frequency (13.56MHz) plasma enhanced chemical vapour deposition (RF PECVD), which has a very low growth rate. In order to increase the growth rate, very high frequency plasma enhanced chemical vapour deposition (VHF PECVD) is used instead. This method has shown a great potential because of its low depo-

sition temperature and high growth rate in preparing high quality $\mu\text{c-Si:H}$ films.^[7-9] The effects of hydrogen dilution and diborane concentration^[10,11] on the properties of films have been widely studied. However, there is little information about the influence of the substrate temperature on the properties. We believe that the substrate temperature is also a critical parameter to determine the growth and the properties of p-type $\mu\text{c-Si:H}$ films and is worthy to carry out a thorough study.

In this paper, we present boron-doped p-type $\mu\text{c-Si:H}$ films deposited at different substrate temperatures. An attempt has been made to ascertain the effect of T_S on the growth and properties of this type of material. Highly conductive films are obtained at low substrate temperatures. The relevant mechanism is also discussed.

2. Experimental details

^{*}Project supported by the State Key Program of Basic Research of China (Grant Nos G2000028202 and G2000028203).

[†]Corresponding author. E-mail: leiqs@yahoo.com

Three sets of samples were deposited on glass substrates by VHF PECVD at a 60MHz frequency in an ultra-high vacuum chamber. A mixture of silane (SiH_4), hydrogen (H_2), and diborane (B_2H_6) was used as a source gas. The samples of Set 1 were deposited at T_S ranging from 90°C to 270°C . The samples of Set 2 and Set 3 were deposited at $T_S=140^\circ\text{C}$ and $T_S=240^\circ\text{C}$, respectively, at diborane concentrations (C_B) ranging from $2.5 \times 10^{-4} \%$ to $12.5 \times 10^{-4} \%$. C_B is defined as $C_B = F_{\text{B}_2\text{H}_6} / (F_{\text{B}_2\text{H}_6} + F_{\text{SiH}_4} + F_{\text{H}_2})$, where F_{SiH_4} , F_{SiH_4} , and F_{H_2} represent the flow rates of B_2H_6 , SiH_4 and H_2 , respectively. The main deposition parameters are listed in Table 1.

The thickness was measured by a Tencor Alpha-step 500 profilometer, and is about 300 nm for the films of Set 1, and about 20 nm for the films of Set 2 and Set 3. The deposition rate was determined by the thickness divided by the deposition time.

Table 1. The deposition parameters of boron-doped $\mu\text{c-Si:H}$ thin films. P_W is the plasma power and P is the total gas pressure.

| Set number | $F_{\text{H}_2}/\text{sccm}$ | $F_{\text{SiH}_4}/\text{sccm}$ | $C_B/10^{-4}\%$ | P_W/W | P/Pa | $T_S/^\circ\text{C}$ | Thickness/nm |
|------------|------------------------------|--------------------------------|-----------------|----------------|---------------|----------------------|--------------|
| 1 | 119 | 1.2 | 5.8 | 10 | 100 | 90–270 | 300 |
| 2 | 119 | 1.2 | 2.5–12.5 | 10 | 100 | 140 | 20 |
| 3 | 119 | 1.2 | 2.5–12.5 | 10 | 100 | 240 | 20 |

3. Results

3.1. Deposition rate

The dependence of deposition rate (R_d) on substrate temperature is shown in Fig.1, where we can

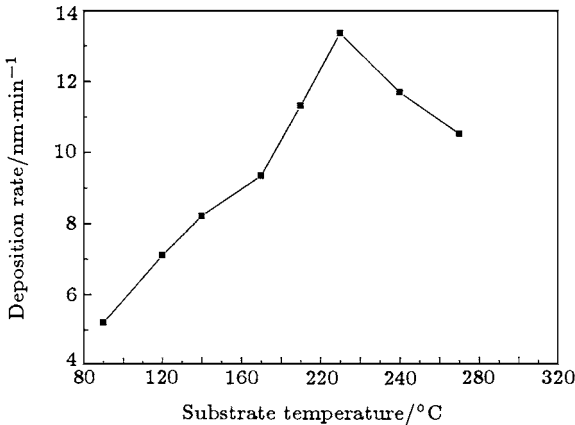


Fig.1. Variation of deposition rate with substrate temperature.

observe that the deposition rate increases with T_S at first. The maximum deposition rate is about 13.3 nm/min at $T_S=210^\circ\text{C}$. With T_S increasing further, the deposition rate begins to decrease. In general, temperature is a critical parameter that affects

The electrical properties such as dark conductivity and Hall effect were measured. σ_d was measured in a range of temperatures from 20°C to 200°C using coplanar Al contacts. Activation energy (E_a) was calculated from the slope of the Arrhenius plot (logarithmic value of conductivity versus T^{-1}). Hall effect measurements were performed at room temperature in a van der Pauw contacts configuration^[12] by using an Accent HL5500 Hall measurement equipment.

To study the crystallinity of the films, Raman spectra were measured in a back-scattering configuration using a Raman spectrometer with a He-Ne laser exciting source. A 5.0 mW output power and 632.8 nm wavelength were used in the measurements. An x-ray diffractometry (XRD) with a $\text{CuK}\alpha$ radiation source was employed to determine the orientations of the crystallites.

the nucleation, the growth of films, and the deposition rate. The dependence of R_d on T_S is associated with the film precursors (such as SiH_3 radicals) reacting with the surface dangling bonds. The detailed analysis is given later.

3.2. Dark conductivity and activation energy

Figure 2 illustrates both the dark conductivity (σ_d) at room temperature and the activation energy (E_a) as a function of T_S . From the figure, we can observe that both σ_d and E_a are strongly dependent on T_S . At a low T_S (90°C), σ_d is relatively low ($\sim 0.268 \text{ S}\cdot\text{cm}^{-1}$) and E_a is high ($\sim 0.067 \text{ eV}$). With T_S increasing up to 190°C , σ_d increases by about two orders of magnitude, reaching a maximum value of $12.54 \text{ S}\cdot\text{cm}^{-1}$, whereas, E_a decreases down to 0.03 eV . When T_S increases further, σ_d decreases accompanied by an increase in E_a . In particular, at $T_S > 210^\circ\text{C}$, the dark conductivity decreases abruptly and drops down to $4.73 \times 10^{-4} \text{ S}\cdot\text{cm}^{-1}$ at $T_S=270^\circ\text{C}$; correspondingly, E_a increases up to 0.243 eV . Such large variations indicate a substantial structural change in the material. It is known that the dark conductivity is determined by the carrier concentration and drift mobility. Increas-

ing T_S would result in a change in structure, leading to a change in carrier concentration. The structural properties of the films, and the change in carrier concentration are given in the next paragraphs.

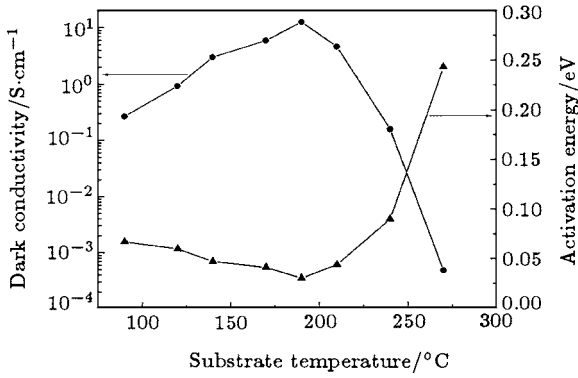


Fig.2. Variations of dark conductivity and its activation energy with T_S .

3.3. Crystallinity

The degree of crystallinity in the films was investigated by Raman studies. Figure 3 shows the Raman spectra of samples deposited at different temperatures T_S (Set 1). For a comparison, all the Raman spectra are shifted by the subtraction of base line. The relationship between the crystallinity and T_S can be observed in the figure. At $T_S \leq 240^\circ\text{C}$, the films are in the microcrystalline phase characterized by crystalline peaks. The sample deposited at $T_S=90^\circ\text{C}$ shows a crystalline peak at about 514cm^{-1} . With T_S increasing, a shift of Raman peak towards higher wavenumbers is observed. At $T_S=170^\circ\text{C}$, the peak is at the highest wavenumber ($\sim 520\text{cm}^{-1}$). With T_S increasing further, the crystalline peak shifts to lower wavenumbers accompanied by a decrease in intensity. At $T_S=240^\circ\text{C}$, both a small shoulder of amorphous fraction at about 480cm^{-1} and a peak of crystalline phase at 508cm^{-1} are observed. When T_S increases up to 270°C , the film is predominantly amorphous indicated by a broad band peaked at about 480cm^{-1} . This phenomenon demonstrates the transition from $\mu\text{c-Si:H}$ to a-Si:H during the film growth. The shift of the crystalline peak to lower wavenumbers, as compared with 520cm^{-1} in c-Si, is attributed to crystalline size effect and stress within the material.^[13,14] For example, the peak at about 510cm^{-1} is due to the presence of tensile strained Si-Si bonds in defective regions.^[15,16]

The transverse optical (TO) phonon mode of the Raman spectra was deconvoluted into three Gaussian peaks corresponding to the crystalline peak ($\sim 520\text{cm}^{-1}$), the amorphous peak ($\sim 480\text{cm}^{-1}$) and the intermediate peak ($\sim 510\text{cm}^{-1}$).^[17,18] The crys-

talline volume fraction (X_c) was calculated from $X_c=(I_c+I_m)/(I_c+I_m+I_a)$,^[19] where I_c , I_m and I_a are the integrated intensities of the crystalline, intermediate, and amorphous peaks respectively. Figure 4 shows the deconvoluted spectrum of the sample deposited at 90°C . X_c estimated from the Raman spectrum is plotted in Fig.5. For the sample deposited at $T_S=90^\circ\text{C}$, X_c amounts to 45%. With T_S increasing, X_c increases gradually and reaches a value of 81% at $T_S=140^\circ\text{C}$. As T_S increases further, X_c decreases and drops down to about zero at 270°C . One interesting phenomenon is that the variation of X_c with T_S is not fully consistent with that of the electrical properties. The maximum σ_d is obtained at $T_S=190^\circ\text{C}$ (Fig.2), while the highest crystalline volume fraction of 81% is obtained at $T_S=140^\circ\text{C}$ (see Fig.4). This result suggests that the electrical properties are determined not only by X_c but also by other factors such as the defect density or stress in the films.

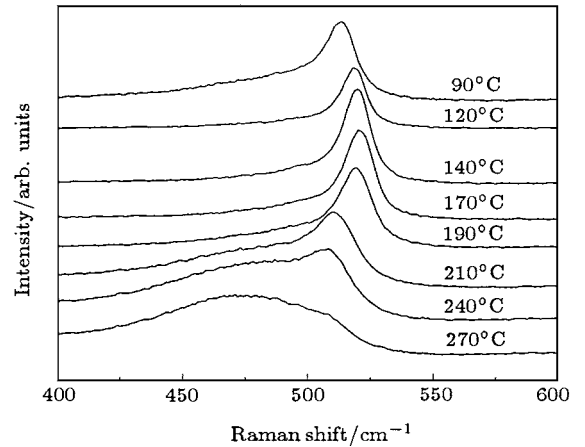


Fig.3. Raman spectra of the boron-doped $\mu\text{c-Si:H}$ films deposited at different temperatures T_S .

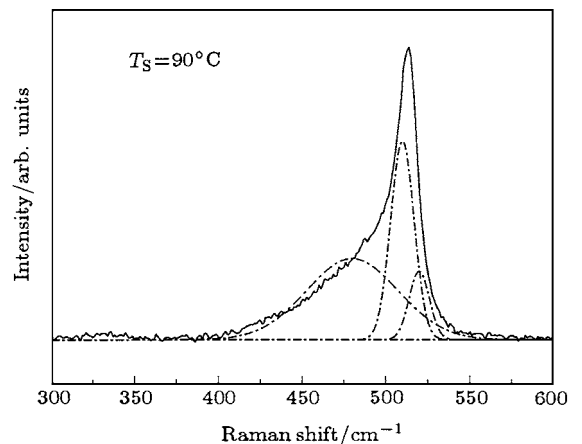


Fig.4. Deconvoluted Raman spectrum of the boron-doped $\mu\text{c-Si:H}$ film deposited at $T_S=90^\circ\text{C}$ showing the crystalline (520cm^{-1}), intermediate (510cm^{-1}), and amorphous (480cm^{-1}) phases.

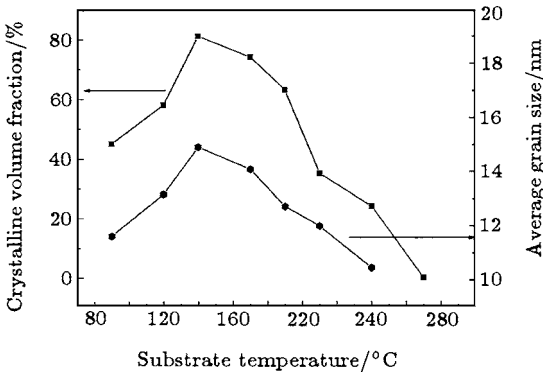


Fig.5. Variations of the crystalline volume fraction and grain size with T_S .

3.4. Grain orientation and grain size

In Fig.6 x-ray diffraction spectra of samples prepared at different temperatures T_S are shown. For samples deposited at $T_S < 240^\circ\text{C}$, diffraction peaks corresponding to the (111), (220) and (311) planes are observed to have a preferential orientation of (111). With T_S increasing, the intensities of these peaks increase first and then decrease, suggesting the change of the crystallinity in the films. The film deposited at $T_S=140^\circ\text{C}$ shows the largest intensities and the smallest full width at half-maximum (FWHM) of the diffraction peaks, indicating that this sample has the highest volume fraction of crystallinity and the largest grain size. The result accords with the Raman spectra. At $T_S=270^\circ\text{C}$, the spectrum shows a small peak at about 28° , which may be due to the nanocrystallites embedded in the amorphous matrix.

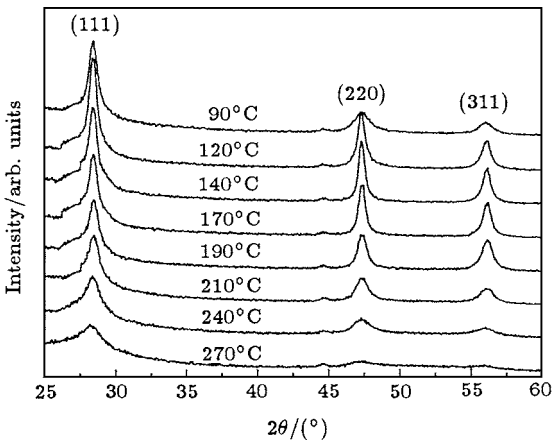


Fig.6. XRD spectra of the boron-doped $\mu\text{c-Si:H}$ films deposited at different temperatures T_S .

The grain size, d_c , was calculated from the (111) peak using the Scherrer formula^[19] and it is $d_c = k\lambda/\beta \cos\theta$, where k (taken as 0.9 in our study) is a constant determined by the geometry of the crystallite, λ is the wavelength of the x-ray radiation, β is the full width of the diffraction angle (2θ) at half-maximum of a diffraction peak. The grain size as a function of T_S is shown in Fig.5, where we can see that the change of the crystalline grain size is consistent with that of X_c . The grain size varies from 10.4 nm to 14.9 nm, depending on the substrate temperature. The maximum grain size is obtained at $T_S=140^\circ\text{C}$.

3.5. Carrier concentration and Hall mobility

Besides the conductivity, another important electrical parameter that determines the use of $\mu\text{c-Si:H}$ films in device applications is the carrier's mobility. The dark conductivity, which shows the non-monotonic dependence on T_S , is determined by the carrier concentration (N_h) and drift mobility. Figure 7 shows N_h and Hall mobility (μ_τ) measured at room temperature of the samples deposited at different temperatures T_S . From the figure, we can see that the carrier concentration and the Hall mobility show a similar dependence on T_S . The films prepared at the lowest T_S (90°C) have $\mu_\tau \approx 0.179 \text{ cm}^2 \cdot \text{V}^{-1} \cdot \text{s}^{-1}$, and $N_h \approx 2.1 \times 10^{18} \text{ cm}^{-3}$. With the increase of T_S , μ_τ and N_h increase and reach the maximum values of $1.21 \text{ cm}^2 \cdot \text{V}^{-1} \cdot \text{s}^{-1}$ and $3.99 \times 10^{19} \text{ cm}^{-3}$, respectively, at $T_S=190^\circ\text{C}$. The result suggests that the doping efficiency is increased and the carrier's transport is enhanced with T_S increasing. We propose that this behaviour results from the improvement of the film's quality. However, with T_S increasing further, both μ_τ and N_h decrease. At $T_S=270^\circ\text{C}$, the minimum carrier concentration of $2.92 \times 10^{16} \text{ cm}^{-3}$ and Hall mobility of $0.0962 \text{ cm}^2 \cdot \text{V}^{-1} \cdot \text{s}^{-1}$ are obtained. The behaviours of μ_τ and N_h are consistent with those of σ_d . In addition, it is noticed that the maximum carrier concentration and Hall mobility are not obtained at the maximum X_c . This result implies that 1) μ_τ and N_h are determined not only by X_c but also by other factors such as stress in the film, 2) with T_S increasing, the film's quality is continuously enhanced after the maximum X_c is obtained.

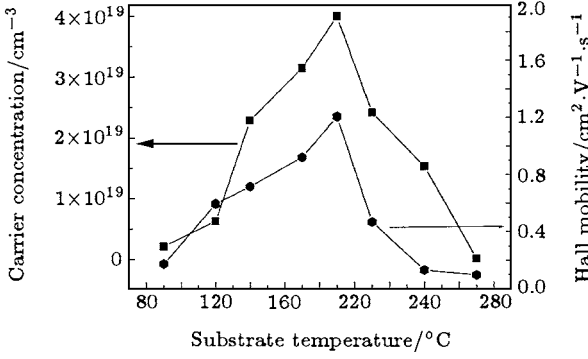


Fig.7. Carrier concentration and Hall mobility of the boron-doped $\mu\text{c-Si:H}$ films versus substrate temperature T_S .

3.6. Influence on the maximum σ_d

For the further understanding of the influence of T_S , two sets of samples were deposited at 140°C and 240°C, separately, at different diborane concentrations (Set 2 and Set 3). The 20-nm-thick films were prepared and dark conductivities were measured for a comparison. Figure 8 shows the variation of dark conductivity with the diborane concentration C_B . The effects of T_S on the variation of σ_d can be clearly observed. At $T_S=140^\circ\text{C}$, as C_B increases from $2.5 \times 10^{-4}\%$ to $8.3 \times 10^{-4}\%$, σ_d increases by about two orders of magnitude, reaching a maximum value of $0.67\text{S}\cdot\text{cm}^{-1}$. With C_B increasing further up to $1.25 \times 10^{-3}\%$, σ_d reduces down to $0.38\text{S}\cdot\text{cm}^{-1}$. However, for films deposited at a higher T_S (240°C), a different variation of σ_d with C_B was observed. In this case, the maximum dark conductivity ($0.233\text{S}\cdot\text{cm}^{-1}$) is obtained at the minimum C_B . With C_B increasing, σ_d decreases monotonically from $0.233\text{S}\cdot\text{cm}^{-1}$ to $0.00347\text{S}\cdot\text{cm}^{-1}$. So, at a lower substrate temperature T_S , a higher diborane concentration C_B is required to obtain a maximum dark conductivity.

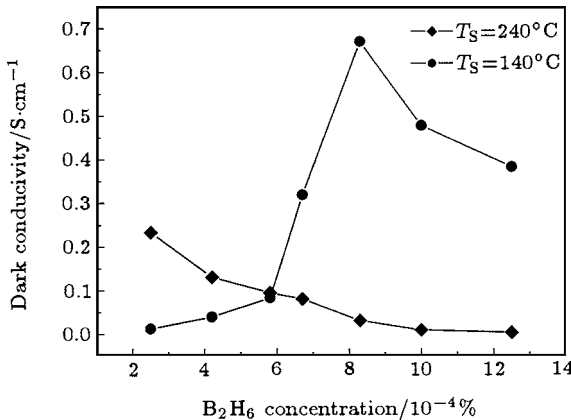


Fig.8. Dark conductivity of the boron-doped $\mu\text{c-Si:H}$ films deposited at $T_S=140^\circ\text{C}$ and $T_S=240^\circ\text{C}$ versus diborane concentration.

4. Discussion

Our experimental results show that the growth rate, the electrical and structural properties of boron-doped $\mu\text{c-Si:H}$ films are all strongly dependent on T_S . We propose that the influence of T_S on the properties results from its influence on the growth processes. The growth species of $\mu\text{c-Si:H}$ films are generally believed to be the SiH_3 radicals,^[20–22] which come from the dissociation of the source gas SiH_4 in plasma. In the growth processes, boron dopant atoms react with Si grains and form B–Si bonds. Also, B atoms can react with H atoms to form B–H–Si and B–H complexes.

In the PECVD deposition process, the growing film surface is heated, accompanied with the thermal desorption of surface bonded hydrogen, which leads to the creation of dangling-bonds on the growing surface.^[23,27] Some of the SiH_3 radicals from plasma move towards the growing surface, and then connect onto the dangling bonds to form Si–Si bonds, resulting in the growing of films. In the mean time, part of the SiH_3 radicals are desorbed from the surface. Thus, the deposition process is influenced by the dangling bonds on the growing surface and SiH_3 radicals that can effectively react with the sites of dangling bonds. During a low substrate temperature deposition, the mobility of precursors on the growing film surface is low, resulting in films with low crystalline fraction and small grain size,^[24] which in turn limits the carrier mobility. Also, in the case of low T_S deposition, large part of boron in crystallites is passivated by hydrogen in the form of B–H–Si bonds,^[25] leading to a low carrier concentration in the film. Thus, at low T_S , the deposited films have the low X_c , N_H , μ_τ and σ_d , which was confirmed by our structural and Hall effect measurements. With T_S increasing, the film-precursor mobility and impurity-atom mobility increase. The increase in mobility of precursors on the growing surface results in a higher crystalline fraction in the films, which in turn enhances the carrier mobility and doping efficiency. The impurity atoms with the mobility increased would have more chance of reacting with the growing precursors, leading to the formation of more B–Si bonds and greater carrier concentrations in the films. In addition, at a higher T_S , a large number of dopants in the films are activated, giving rise to an increase in carrier concentration. So, with T_S increasing, the film's quality is improved and both N_H and μ_τ increase, resulting in an increase in dark conductivity. Also, with T_S increasing, the surface dangling

bonds are increased.^[26] Thus, more precursors would find sites to be connected onto, leading to the increase in deposition rate.^[27] However, with T_S increasing further, when T_S exceeds 190°C , the crystallinity, N_H , μ_τ and σ_d decrease continually. We believe it is due to the unfavoured thermal CVD of diborane, which is chemically unstable and can deteriorate the properties of the film. At $T_S > 210^\circ\text{C}$, although the dangling bonds continue to increase in number, there are not enough SiH_3 precursors to react with all surface reaction sites. In addition, the SiH_3 radicals on the growing surface decrease in number continuously because of the thermal desorption, leading to a decrease in deposition rate.

It can be seen from Fig. 8 that at a low T_S (140°C), in order to reach a maximum σ_d value, a higher B_2H_6 concentration is needed.

5. Conclusion

The effects of substrate temperature on the

growth and properties of boron-doped $\mu\text{c-Si:H}$ films are investigated. Results suggest that the growth rate, the structural and electrical properties of the samples are all strongly dependent on T_S . With the increase of T_S , the growth rate increases initially and then reaches a maximum value of 13.3 nm/min at $T_S=210^\circ\text{C}$. Structural analysis shows that the crystallinity and the grain size increase initially and then decrease. The samples deposited at low T_S are shown to possess a low dark conductivity and high activation energy. With T_S increasing, σ_d increases accompanied with the decrease in E_a . At $T_S=190^\circ\text{C}$, a high dark conductivity of $12.54\text{ S}\cdot\text{cm}^{-1}$ is obtained. With T_S increasing further, σ_d decreases and drops down to a minimum value at $T_S=270^\circ\text{C}$. Hall effect measurements suggest that N_h and μ_τ have a similar dependence on T_S . Both N_h and μ_τ reach their maximum values at $T_S=190^\circ\text{C}$. In addition, it is observed that at a lower T_S , a higher diborane concentration is required in order to obtain a maximum dark conductivity.

References

- [1] Guha S, Yang J, Nath P and Hack M 1986 *Appl. Phys. Lett.* **49** 218
- [2] Ferreira G M, Chi Chen, Koval R J, Pearce J M, Wronski C R and Collins R W 2004 *J. Non-Cryst. Solids* **338-340** 694
- [3] Saleh R and Nickel N H 2003 *Thin Solid Films* **427** 266
- [4] Gordijn A, Rath J K and Schropp R E I 2004 *J. Non-Cryst. Solids* **338-340** 110
- [5] Sasaki T, Fujikake S, Tabuchi K, Yoshida T, Hama T, Sakai H and Ichikawa Y 2000 *J. Non-Cryst. Solids* **266-269** 171
- [6] Kondo M, Nasuno Y, Mase H, Wada T and Matsuda A 2002 *J. Non-Cryst. Solids* **299-302** 108
- [7] Rath J K, Walling J and Schropp R E I 1996 *Mater. Res. Soc. Symp. Proc.* **420** 271
- [8] Shi J J, Huang S Y, Chen K J, Huang X F and Xu J 2001 *Chin. Phys.* **10** 748
- [9] Concari S B and Buitrago R H 2004 *J. Non-Cryst. Solids* **338-340** 331
- [10] Chen H, Gullanar M H and Shen W Z 2004 *J. Cryst. Growth* **260** 91
- [11] Das D and Jana M 2004 *Mat. Lett.* **58** 980
- [12] Le Comber P G, Jones D I and Spear W E 1977 *Philos. Mag.* **35** 1173
- [13] Iqbal Z and Vebrek S 1982 *J. Phys. C* **15** 377
- [14] Saha S C and Ray S 1995 *J. Appl. Phys.* **78** 5713
- [15] Kanekon T, Wakagi M, Onisawa K and Minemura T 1994 *Appl. Phys. Lett.* **64** 1865
- [16] Furukawa S and Mayasato T 1988 *Phys. Rev. B* **38** 5726
- [17] Veprek S, Sarott F A and Iqbal Z 1987 *Phys. Rev. B* **36** 3344
- [18] Kaneko T, Wakagi M, Onisawa K and Minemura T 1994 *Appl. Phys. Lett.* **64** 1865
- [19] Findeisen E, Feidenhans'l R, Vigild M E, Clausen K N, Hansen J B, Bentzon M D and Goff J P 1994 *J. Appl. Phys.* **76** 4636
- [20] Gallagher A 1988 *J. Appl. Phys.* **63** 2406
- [21] Matsuda A and Tanaka K 1987 *J. Non-Cryst. Solids* **97** 1367
- [22] Matsuda A, Nomoto K, Takeuchi Y, Suzuki A, Yuuki A and Perrin J 1990 *J. Surf. Sci.* **227** 50
- [23] Zhang X D, Zhao Y, Gao Y T, Zhu F, Wei C C, Sun J, Geng X H and Xiong S Z 2005 *Acta Phys. Sin.* **54** 3910
- [24] Yamaguchi M and Morigaki K 1999 *Philos. Mag. B* **79** 387
- [25] Sah Chih-Tang, Sun Jack Yang-Chen and Tzou Joseph Jeng-Tao 1984 *J. Appl. Phys.* **55** 1525
- [26] Robertson J and Powell M J 1999 *Thin Solid Films* **337** 32
- [27] Chandan Das, Arup Dasgupta, Saha S C and Swati Ray 2002 *J. Appl. Phys.* **91** 9401